FABRICATION OF THE TRANSITION SECTION OF A CORRUGATED WAKEFIELD ACCELERATOR VIA LASER MICROMACHINING*

P. Bado†, M. A. Dugan, and A. A. Said, Translume, Inc., Ann Arbor, MI, 48108, USA
S. Siy, K. Suthar, A. Zholents, Argonne National Laboratory, Lemont, IL, 60439, USA

Abstract

A wakefield accelerating structure is being designed to facilitate sub-terahertz Čerenkov radiation. This accelerating structure consists of several sections of internally corrugated tubes, that are coupled together using transition sections. The fabrication of these transition sections is presented. Modelling of various fabrication errors was undertaken to understand their effect and to determine fabrication tolerances. Source of machining imperfections are reviewed and their impact compared to the modelling results.

INTRODUCTION

A cylindrical, corrugated wakefield accelerating (CWA) structure [1] is being developed to create sub-terahertz Čerenkov radiation produced by an electron bunch. The accelerating structure consists of several copper-based, 50-cm long, sections of internally corrugated tubes with a 1-mm inner-radius. These elements are coupled together using ultra-compact transition sections, as shown in Fig. 1, which are also copper-based.
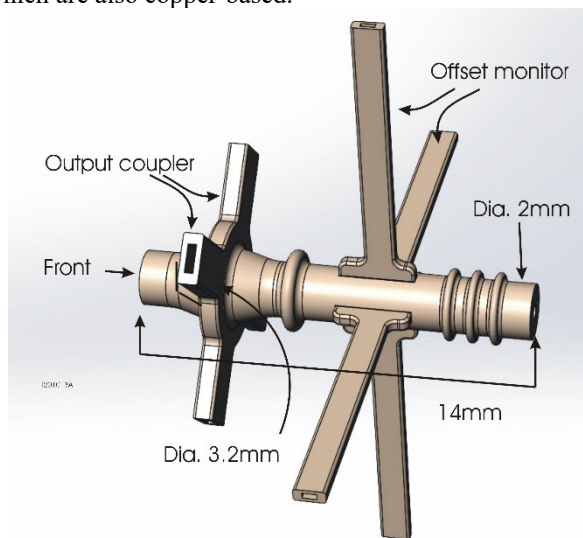
Figure 1: Model of the inner volume of a transition section, with main dimensions.

Beside their mechanical and vacuum coupling functions, these transition sections provide a means to monitor the centering of the electron bunch, and to couple out unused energy in the TM01 accelerating mode from the corrugated

waveguide while allowing the TE11 transverse mode to pass through. The output coupler is expected to extract on the order of a kilowatt of power.

FABRICATION APPROACH

The fabrication is divided into four main steps: First, a fused silica glass mandrel is fabricated. Its external shape corresponds to the internal volume of the transition section. Second, a thin layer of Gold is sputtered onto the surface of this glass mandrel, and subsequently a thick copper layer is electro-deposited on top of the gold. Third, the glass mandrel that is at the core of this assembly is etched away, leaving a hollowed copper shell with the desired internal geometry; and finally secondary machining operations, such as milling and drilling, generate the external end faces and other reference surfaces required for the integration of the transition section into the general CWA structure.

The first step – the fabrication of the sacrificial fused silica glass mandrel- is based on a sequential combination of laser irradiation and chemical etching [2], as illustrated in Fig. 2. Shape-contouring is introduced by illuminating a defined pattern with a laser generating ultrashort pulses. The pulse energy is set sufficiently low to avoid ablation, yet high enough to locally modify the short-range ordered fused silica molecular matrix.
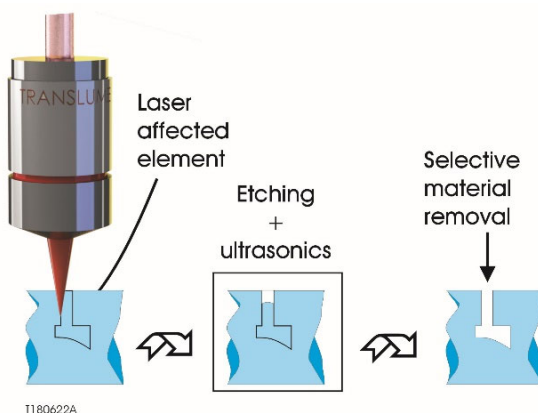
Figure 2: The two-step glass shaping process - Laser direct write, followed by selective etching.

With the proper processing parameters, the laser-exposed volume elements (*i.e.* voxels) etching susceptibility is greatly increased. This localized enhanced etching is used to shape the desired glass part geometry. One of the key metrics associated with this part of the fabrication process is the ratio of the etching rate of the laser-exposed voxels versus the etching rate of the virgin fused silica glass. Under optimized conditions this etching ratio can exceed 100:1, but it degrades rapidly with the depth of the laser processing.

FABRICATION DETAILS

The transition section has a central body with a rotational geometry, and two sets of four waveguides that are perpendicular to the main axis. The main body diameter ranges from 2 mm to 3.2 mm (not including the two sets of orthogonal waveguides) and the length is approximately 14 mm. These various dimensions correspond to the inner geometry of the final copper interface section. Due to spatial and temporal aberrations, the intensity and the shape of the laser focal spot change drastically with the depth of the laser processing. This limits the depth of the laser writing to approximately 3.5 mm. The transition section has dimensions that exceed this limit. To address this issue, the transition section is divided into several sub-units that independently fit in the machinable volume.

Initially the transition section was divided in a main cylindrical section, to which lateral waveguides were subsequently attached (either in group or separately) using an epoxy, as illustrated in Fig. 3. With this fabrication approach, the cylindrical section main axis rested perpendicular to the laser writing beam. The lateral waveguides were written separately, and they were subsequently epoxied to the main body. This approach resulted in relatively large errors exceeding the maximum allowable tolerances, as defined from simulations. Several sources of errors were identified: The epoxy thickness could not be reproducibly controlled; the etching ratio was poor (this is indirectly related to the cylindrical section main axis being perpendicular to the laser axis); and the lateral waveguides could not be aligned accurately with the device main axis.
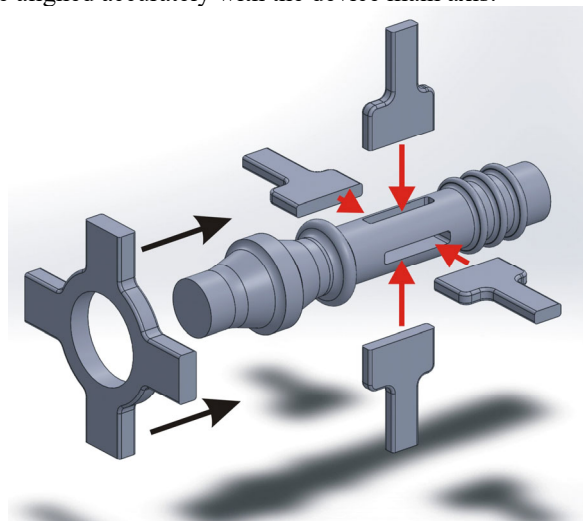
Figure 3: Exploded schematic view of a transition unit consisting of a central cylindrical into which waveguides are attached.

The division of the transition section into sub-elements was modified to address these issues. Shorter sections that can be fabricated with the laser axis parallel to the sub-elements central axis are now used. The various elements are no longer epoxied. Rather they are mechanically held together during the sputtering and the electroforming. The lateral waveguides are fabricated as stand-alone units comprising all four arms.

This approach offers a fair amount of flexibility as to where the divisions between the various subunits are located. However, due to the height restrictions discussed above, numerous sub-elements are required. Several configurations are being explored. In one configuration, the transition element is divided into twelve main elements, some of which have identical geometry but different lengths, as shown in Fig. 4. Once the various fused silica glass sub-elements have been fabricated, the transition section is assembled by sliding them onto a precision-machined stainless steel pin. This master pin forms the backbone of the assembly. It provides the main mechanism to insure concentricity between the sub-elements. During the ensuing fabrication steps, the sub-elements are held tightly together using jigs with compression springs.
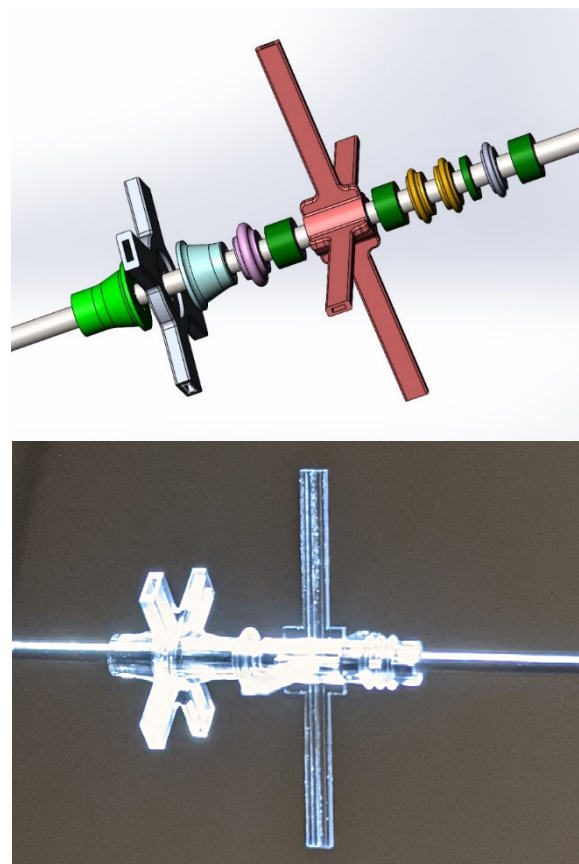
Figure 4: (Top) Exploded schematic view of a transition unit consisting of twelve glass elements and one metal pin. (Bottom) Corresponding assembled glass demonstrator.

Modelling of the transition section was used to determine the maximum acceptable fabrication deviations from the design intent. The impact of any waveguide offsetting was studied for both the TM01 coupler and the beam offset monitor. Based on this simulation, it is estimated that the maximum acceptable TM01 coupler lateral offset is $50\,\mu$m. The system is more susceptible to offsets along the main (Z-) axis.

The impact of concentric misalignments (radial shift) between adjacent elements forming the transition section was also modelled, as shown in Fig. 5.
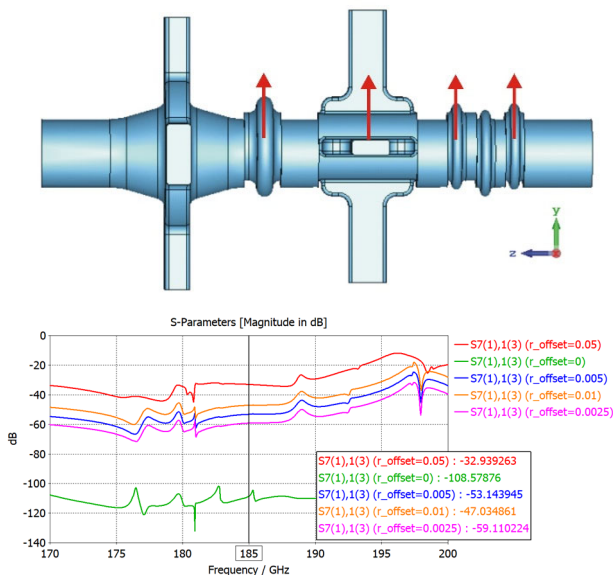
Figure 5: (Top) Schematic view showing radial offsets between adjacent elements of the transition section. (Bottom) TE11 Isolation from TM01 as function of radial offset.

The total radial offset between adjacent sections should not exceed 10 microns.

Deviations from the design intent are associated with various parts of the fused silica glass elements: While the stages moving the substrate have a positioning accuracy that is better than 1 micron, the change of the laser spot shape with the depth of the laser processing results in larger dimensional nonconformities. The etching process introduces further divergences from the design intent. These are related to the time it takes for the etchant to reach a given voxel. This is a strong function of the depth of the feature and the local geometry. However, these etching and focal spot deviations are reproducible, and through trial and error can be mostly compensated, as illustrated in Fig. 6. We project that the residual errors due to the laser writing and the etching will be less than 10 microns for any critical dimensions of any given sub-element.

Design element	Diameter Micron	GEN_1 Micron	GEN_2 Micron	GEN_3 Micron
A	1,000	953	999	1,002
B	1,000	982	1,022	1,008
C	1,068	1,063	1,101	1,080
D	1,333	1,326	1,355	1,345
E	1,621	1,589	1,628	1,624
F	1,621	1,580	1,620	1,622
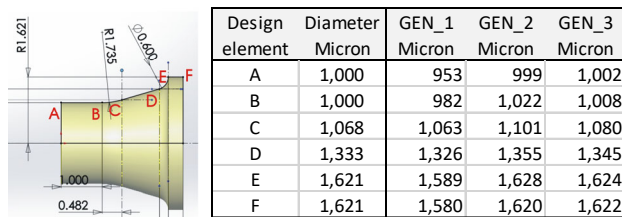
Figure 6: (Left) Drawing of one of the transition section's elements. (Right) Metrology data from successive device.

The diameter of the central hole (used for the alignment pin) is the most critical dimension, and the etching is stopped once this diameter reaches a predetermined value. The associated dimensional error is less than 3 microns. Radial offsets (Fig. 7) are held below the 10-μm limit established from simulations.

The length of each element (along the central axis) is presently adjusted by selecting a fused silica substrate of

the proper thickness. This introduces another source of error. To minimize its impact, the number of glass elements is being reduced through the combination of shorter adjacent ones. This part reduction effort will also eliminate other imperfections.
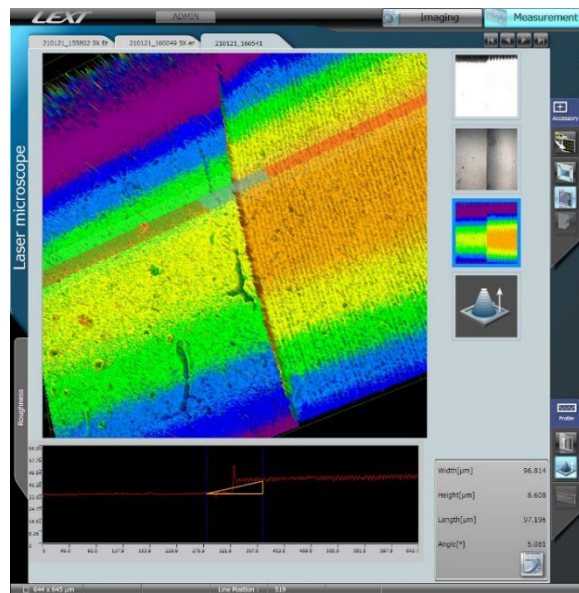
Figure 7: Radial offsets between adjacent sub-elements.

Subsequently a thin layer of Gold is sputtered onto the mandrel. This layer serves as a conductive seed for the copper electroforming. The copper is electrodeposited using a recipe optimized to minimize electric breakdown [3].

CONCLUSION

An ultra-compact transition section of a corrugated wakefield accelerator is fabricated by electro-depositing copper onto a sacrificial fused silica glass mandrel. While a full copper demonstrator has yet to be produced, it appears that the deviations from the design intent associated with the glass mandrel fabrication are within the range established through simulations.

REFERENCES

[1] A. A. Zholents and W. M. Fawley, "Proposal for intense attosecond radiation from an X-ray free-electron laser," *Phys. Rev. Lett.*, vol. 92, no. 22, p. 224, 2004. doi:10.1103/PhysRevLett.92.224801

[2] Y. Bellouard, A. Said, M. Dugan, and P. Bado "Fabrication of high-aspect ratio, micro-fluidic channels and tunnels using femtosecond laser pulses and chemical etching", *Opt. Express,* vol. 12, pp. 2120-2129, 2004. doi.org/10.1364/OPEX.12.002120

[3] S. Kobayashi *et al*., "Electrical breakdown characteristics of electroformed copper electrodes in vacuum", in *Proc. ISDEIV. 19th International Symposium on Discharges and Electrical Insulation in Vacuum* (Cat. No.00CH37041), pp. 41-44 vol.1, 2000. doi: 10.1109/DEIV.2000.877247